Towards quantum dot luminescence enhancement

An investigation of radiative properties of single quantum dots
in close proximity to a nanosize metal object

B.J.C.M. van Gils

Optical Techniques Group
Applied Physics
Department of Science and Technology
University of Twente

Graduation committee
Dr. J. Hernando-Campos
Prof. Dr. N.F. van Hulst
Dr. C. Otto
Dr. M.F. García-Parajó

May 17, 2004

Contents

List of Figures

Chapter 1

Introduction

1.1 Quantum dots

Quantum dots (QDs), semiconductor nanocrystals, artificial atoms; all designate the same type of physical objects; very small, artificially fabricated crystals of semiconductor material. Their sizes range from a few nanometres to tens of nanometres. They partially behave like bulk material and partially like a single giant atom because of their size. Therefore they have unique optical and electronic properties. This thesis will focus on the optical part. Their luminescent emission spectrum is narrow and depends on their material as well as their size. These properties make QD interesting for optical tagging and light generation.

Figure 1.1: QD emission from small (left) to less small (right) [Ene]

1.2 Project description

The project presented in this thesis originated from two recently published articles that report on enhanced luminescence properties of single QDs. They were published by

research groups of Bawendi [SWF$^+$02] and Woggon [KSY$^+$02]. The first article reports on luminescence of individual QDs deposited directly on a sample with a roughened gold surface. The second article focusses on bulk experiments on QDs separated from a gold colloid layer via a space layer. These articles show that the luminescence properties of single QDs can be enhanced in the proximity of nanometric metal particles. Both report enhanced emission intensity up to a factor of 5. Bawendi also reports on linear emission polarisation, reduced blinking and more than 1000 times shorter emission lifetime.

The strength of Bawendi's experiment is that they studied effects on single QDs, giving information about the nonaveraged properties. Unfortunately, the local environment of the QDs studied is not known in his experiment. The article of Woggon's group on the other hand shows a well defined geometry of the experiment, but has as drawback that the QDs are studied in bulk.

In this project we have combined the best of both experiments. The main experimental goal of the project has been:

"To study the distance dependent radiative properties of single quantum emitters in close proximity to a metal nanoparticle"

In this project we have used QDs as single quantum emitters. They are very suited for this type of experiment because their radiative decay is slow, which eases the observation of changes therein; and they show almost no photobleaching, which enables time consuming experiments. Their quantum yield and absorption cross section is comparable to other luminescent systems. Besides that, Bawendi reports on modified photophysical properties of QDs, like blinking, emission dipole and spectra.

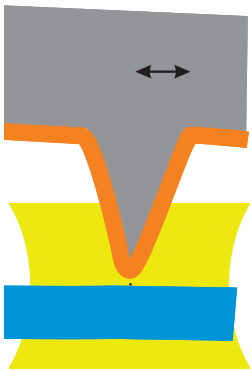

The small black spot represents the QD (5nm), the rectangle below the glass slide. The lighter area shows the size of the focal spot of the microscope scaled to the QD (300nm). The AFM tip above the QD has a scaled tip apex (50nm radius), but in fact is much larger (about 2μm high). The thickness of coating is to scale again (40nm).

Figure 1.2: Experimental setup (sizes roughtly to scale)

The experiment is performed using an inverted confocal microscope used in combination with an atomic force microscope equipped with a gold coated tip. Figure 1.2

gives an idea of the sizes in the experiment. In the experiment the AFM tip is acting as the metal nanoparticle, as well as the probe that gives information on the environment of the QD. The tip is scanning the surface while the QD is kept fixed in the center of the focus. In this way we expect to accurately control the distance between the metal tip and the QD and observe changes in its radiative properties of the QD that correlate with the metal-emitter separation. For experimental details I refer to chapter 3.

1.3 Relevance

Radiative decay engineering is a general term that is used for several processes that influence the properties of luminescent systems, especially their radiative decay rate. Influencing (increasing) this radiative rate of single quantum emitters attracts much research interest since it facilitates better detection of these systems.

Even more interesting is the distance dependent increase of radiative rate to improve optical resolution of microscopes. In optical microscopy the diffraction limits the resolution of imaging. As the radiative rate can be influenced on distances smaller than this limit, this enables the appearance of substructures on a regular diffraction limited spot, which in turn enables improvement of the resolution of the detection apparatus as seen in figure 1.3. Since physicists always try to break limits they face, the research interest in the topic is easily understood.

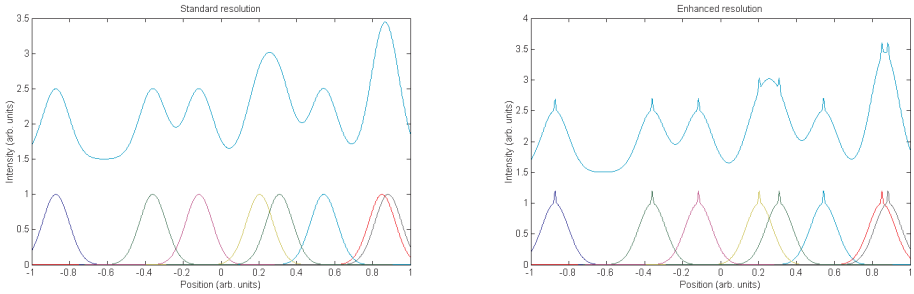

Figure 1.3: Resolution enhancement by distance dependent increase of radiative rate

Besides that, studying these effects on QD is interesting since QDs are potentially much better candidates for tagging biological material compared to conventional luminescent dyes.

In cell research, luminescent dyes are usually used to label regions of the membrane the cell, proteins or other interesting organelles. These dyes enable the investigation of the spread of particles, their number and their position in the cell. Unfortunately, dyes have a broad emission and a narrow absorption spectrum, which makes it difficult to use more than 1 or 2 different types of dye in one experiment and limits the number of different types of particles that can be labelled at the same time. The fast bleaching of

dyes prohibits experiments that that last long time.

The size dependent narrow emission spectrum and broad absorption spectrum of QDs overcomes the multiple labelling problem. One can excite all sized QDs with blue light and discriminate between sizes by recording their emission spectra. Also, QDs are photostable in the sense that they almost never bleach, which enables time consuming experiments.

However, the semiconductor material is toxic and non-water-soluble. To be able to use QDs in biological experiments they have to be encapsulated with a very thin, passivating and water-soluble shell, e.g. silica. This shell also enables the linking to biological material. Unfortunately, it also increases their physical size. Since the size of the active core is not changed, their emission spectrum is not influenced.

Chapter 2

Theory

The theory supporting the experiments is twofold. On the one hand one needs to know about the physics of quantum dots and their luminescence and on the other hand the theory on influencing the radiative decay of luminescent systems.

2.1 Semiconductors

From quantum physics we learn that an atom contains electrons which have discrete energy levels. Such an energy level can contain zero (unoccupied level), one or two (occupied level) electrons. When two or more atoms are brought together to form a molecule, these energy levels are mixed to form new energy levels. The number of energy levels is conserved. When the number of atoms becomes very large, the spacing between these energy levels becomes smaller. Still they are discrete, but their density is that large that we speak of a band of allowed energies. See figure 2.1.

The regularly positioned positively charged atom cores in a crystal create a periodic potential. This periodic potential makes that the energy bands are not continuous from bottom to top, but have several gaps. These gaps are called bandgaps and represent forbidden electron energies in the crystal. (See figure 2.2). In a semiconductor a bandgap is separating the highest (partially) filled band, or valence band, from the lowest unoccupied band (the conduction band). According to the semiclassical model of electron dynamics [AM76] a band that is either completely filled or empty can carry no current. Since the semiconductor has either occupied or unoccupied bands, separated by the bandgap, a semiconductor is not conductive. In a metal on the contrary, this boundary of the filled and empty bands is in a region of allowed energies and so metals are conductive.

A semiconductor sometimes is conductive. This happens when some electrons from the valence band are promoted across the bandgap into the conduction band. This can happen for example when applying electrical potential, heat, or light. The larger the

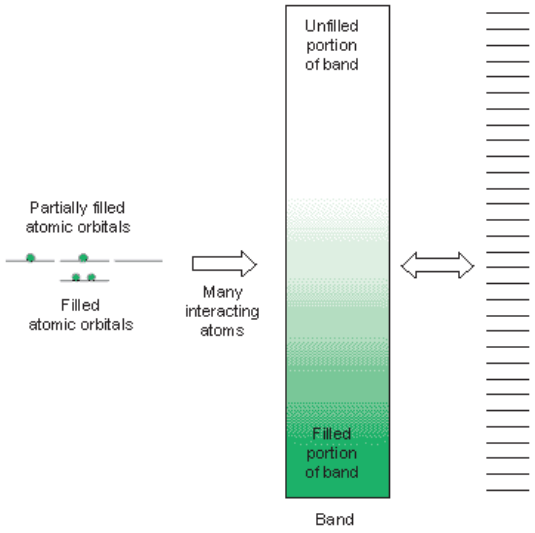

Figure 2.1: Adding more atoms leads to the appeance of an energy band [Qua]

bandgap, the harder it will be to promote electrons from the lower to the higher bands. In bulk semiconductors this bandgap is dependent solely on the material.

2.1.1 Quantum dots

As the size of a real world system is decreased until several (tens of) nanometres in all 3 dimensions, we start talking about quantum dots. They are a real world example of the well known Schrödingers' particle-in-a-box problem. The top part of figure 2.3 shows a potential well. Electron wave functions in this well have to fit the boundary conditions. The result is that electrons will have discrete energies. These energies for a box of depth V_0, width d and electron mass m are given by

$$E_n = -V_0 + \frac{n^2\pi^2\hbar^2}{2md^2}, n = 1, 2, 3, ... \tag{2.1}$$

The figure shows the two lowest energy wave functions that are a solution to the problem. As the potential well becomes deeper, more energy levels will be confined. In the beginning the spacing of levels is large, but this decreases at each solution.

Of course this one dimensional problem is a simplification of the real three-dimensional potential in a quantum dot. The qualitative result however is right and predicts the properties of a quantum dot. In literature there have been analytical as well as numerical studies to more elaborated theory on quantum dot systems. Those have been able to also predict to a good approximation the numerical values of quantum dot properties.

Combining the results of Schrödingers' particle-in-a-box with the bandstructure of a semiconductor, we get a bandstructure as shown in figure 2.4. At the edges of the

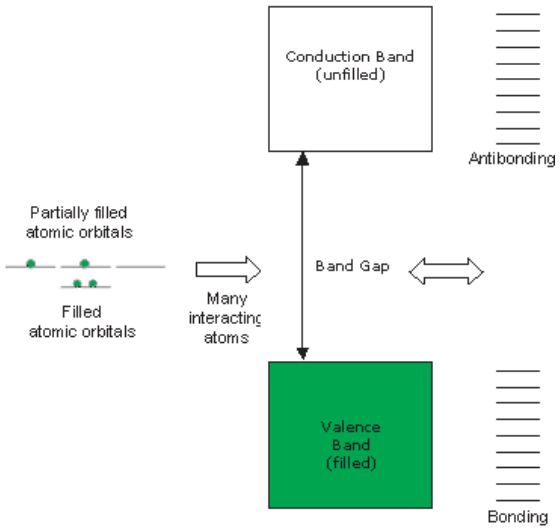

Figure 2.2: A periodic potential creates a bandgap of forbidden energy levels [Qua]

bands, the energies become discrete as a result of the confinement, not only for electrons in the bottom of a band (like the topside of fig 2.3), but also for electrons in the top of a band (bottom side of same figure). In this way the gap between these edge states grows. When the width of the potential well (d of eq. 2.1) is decreased, the spacing of these levels will grow and the size this gap will increase. This is one of the most important properties of quantum dots: The bandgap in quantum dots is dependent on size as well as material.

2.2 Photoluminescence

Photoluminescence is the process of an atom absorbing a photon and re-emitting another at a slightly lower energy, or longer wavelength. This process is graphically represented by a Jablonski diagram as shown in in figure 2.5. In this figure the state S_0 represents the ground state of and atom and the higher S-states excited states of the same system. The blue arrow A represents the atom absorbing a photon. The energy of this photon promotes the atom into a excited state, most probably into an excited vibrational state of this excited state. After the absorption the atom relaxes very fast into the ground excited state via internal conversion by which it loses some energy. After that the atom relaxes back into the ground state by means of emitting a photon with a bit lower energy than the absorbed one, as indicated by the green F arrow.

Also the atom can relax through state T, called a triplet state. Since this process is essentially forbidden, the time it takes to fall back can be long. The last process, relaxing through T_1 is called phosphorescence, in which a photon is emitted at even

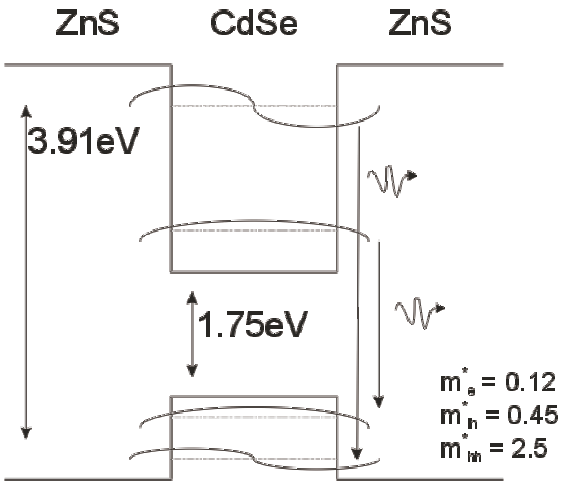

Figure 2.3: Schrödingers' particle in a semiconductor box.

lower energy and at a longer time scale.

Atoms only can absorb photons that have an energy that fits the energy gap between two levels. However, vibrational and rotational excited states make that the excitation can have a distribution of energies. The result is that the absorption is broadened, as shown in figure 2.6. Absorption into different vibrational levels of the excited state combine to a composite absorption spectrum.

On the other hand, if an atom has relaxed into the ground level of the excited state, the electron can fall back into several vibrational levels of the ground state, as shown in figure 2.7. This is the reason that also the emission spectrum of an atom is broadened. Mind that this figure is flipped with respect to the previous.

(The term photoluminescence is used next to luminescence, fluorescence and others. Depending on the timescale and studied systems one of these terms is correct. Throughout this thesis I only will the term 'luminescence'.)

2.2.1 Quantum dot luminescence

In quantum dots electrons are excited from the valence band across the bandgap into the conduction band, as shown in figure 2.2. As it is promoted, the electron leaves an empty place in the band, which is called a hole. The hole and the electron form a exciton which can be modelled like a hydrogen atom. They will attract each other.

Just as with atoms, quantum dots just can absorb radiation that fits a energy gap between a filled state and an empty state. But since the bands consist of very densely spaced energy levels, there are much more combinations of energy levels in the valence- and conduction band that create a certain energy difference. That is why quantum dots have a absorption spectrum that is very broad. As the energy becomes higher more and more potential combinations exist, and therefore the probability of a photon being

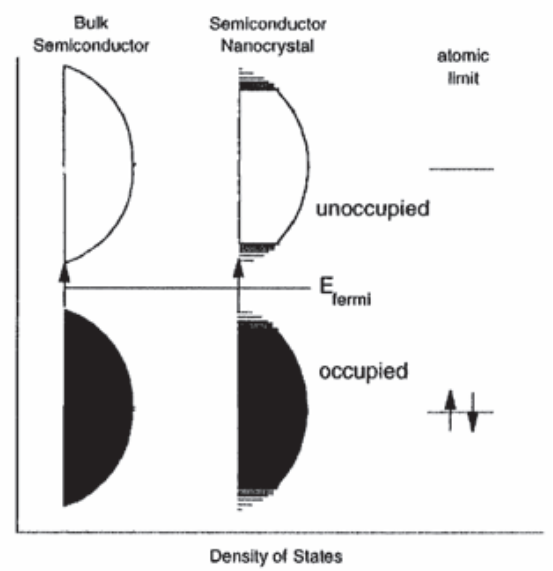

Figure 2.4: The energy bands in a small particle

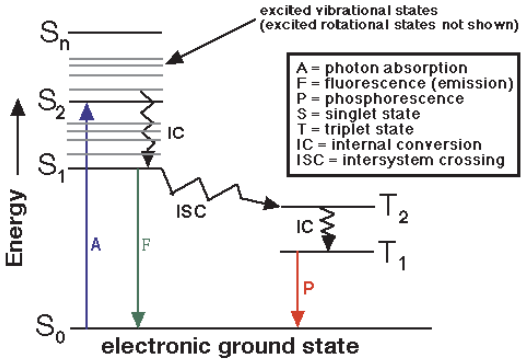

Figure 2.5: Jablonski diagram

absorbed increases. This results in an absorption spectrum shown in figure 2.8. The first and third peak in the spectrum originate different values of n in equation 2.1. The second peak originates from a second effective hole mass (m_h) in equation 2.2.

On the other hand, from quantum mechanics it can be derived that the transition from a non-vibrational/rotational excited state to the non-vibrational/rotational ground state is highly preferable. This means that an electron in an excited vibrational or rotational state has to relax to the ground excited state, and from there only relaxes back into the ground-ground state, unlike the atom-case. This means that the energy that is released in this process is defined very well and the emission spectrum is very narrow! This is shown in figure 2.8.

This makes QD's very interesting from the spectral point of view. While atoms have

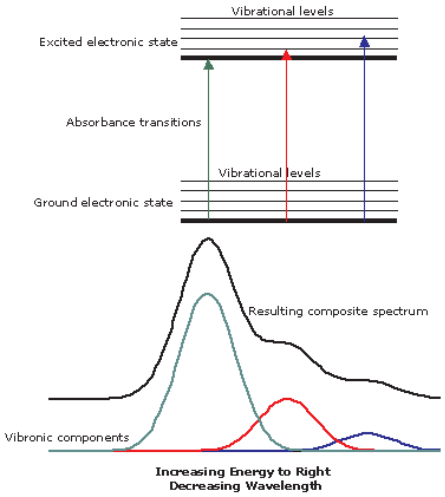

Figure 2.6: Absorption spectrum broadening of a luminescent atom [Qua]

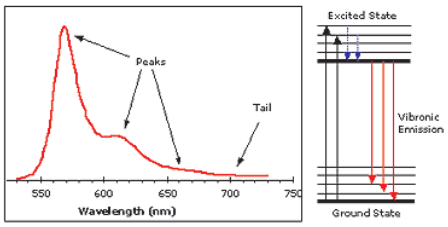

Figure 2.7: Emission spectrum broadening of an atom.[Qua]

a mirrored absorption - emission spectrum, quantum dots can be excited from the blue light until the emission wavelength and their emission spectrum will be narrowed and symmetrical around the central wavelength.

As mentioned in section 2.1.1 (fig. 2.3) the bandgap in quantum dots is dependent on their size as well as on the material. This means that by changing the size of the quantum dots, also will the width of the bandgap. Since the energy of emitted photons is directly related to the width of the bandgap, also the emission spectrum will depend on size.

Equation 2.1 forms the basis of the energy of the emitted light. A detailed, but still elementary study [Bru84], approximates the energy of the lowest excited state by studying a perfect spherical particle, using the effective mass model. This paper shows that the energy of the lowest excited state becomes approximately:

$$E = \frac{\hbar^2 \pi^2}{2R^2}\left[\frac{1}{m_e} + \frac{1}{m_h}\right] - \frac{1.8e^2}{4\pi\epsilon R} \tag{2.2}$$

Where R is the particle radius, $m_e(m_h)$ the electron (hole) effective mass and ϵ dielectric constant of the material involved. Because of the approximations used, this ap-

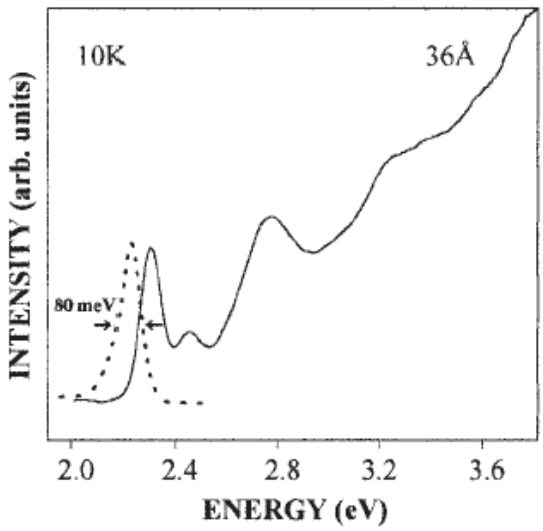

Figure 2.8: Absorption and emission spectrum from a quantum dot. [ENSB99]
Emission spectrum (dotted) and absorption spectrum (solid). The peaks in the absorption spectrum are clarified in the text.

proximation is valid for particles down to a radius of about 3nm. The group of Bawendi has established an experimental curve to couple particle diameter d in nanometres and to the maximum exciton absorption wavelength in nanometres:

$$d = \frac{1 - 3.8121 \times 10^{-4}\lambda}{-0.79196 + 9.5125 \times 10^{-4}\lambda} \tag{2.3}$$

Figure 2.9 shows that indeed the theoretical curve is deviating from the experimental below particle radii of 3nm.

Summarizing; quantum dots have a tunable emission spectrum and a broad absorption spectrum. Therefore they are especially interesting as markers in multiple labelling experiments. In particular CdSe are interesting (see fig. 2.10) because their emission wavelength can be tuned throught almost the entire visible spectrum.

Luminescence lifetime and quantum yield

Promoting an electron from the valence band to the conduction band, an electron-hole pair or an exciton, is formed. Exciton radiative decay has a longer lifetime than radiative decay of atoms. For quantum dots values are in the regime of tens of nanoseconds. Ideally QDs have single exponential decay, but the QD also can decay via pathways offered by surface defects. This results in shorter lifetimes that are observed next to the longer exciton decays.

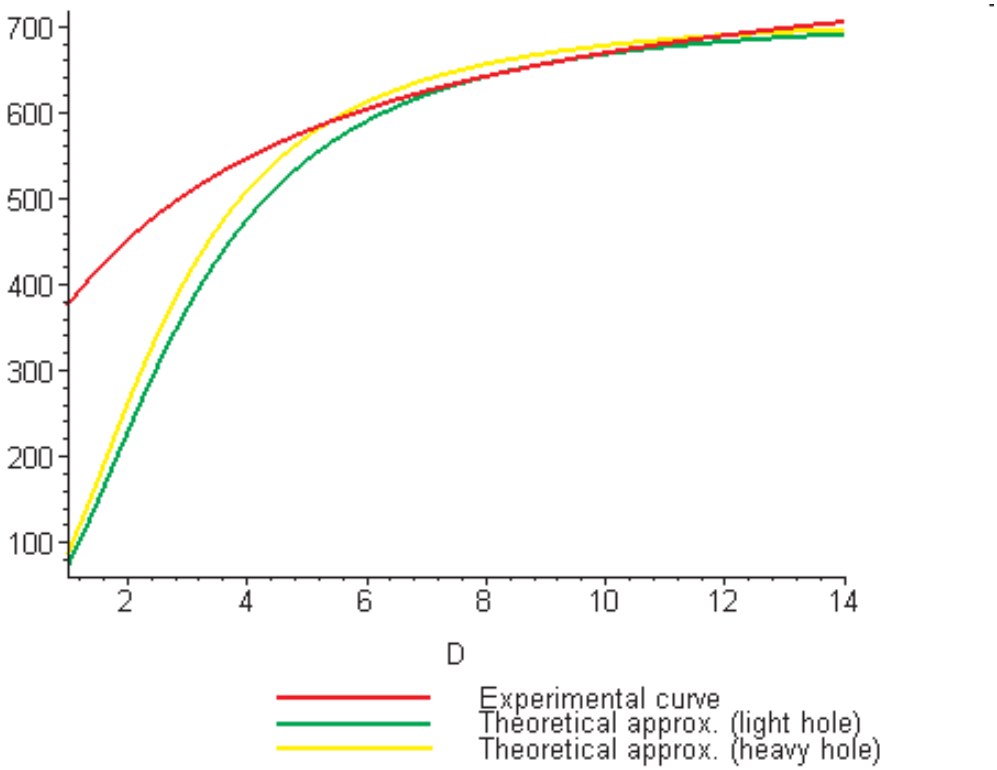

Figure 2.9: Theoretical and experimental curves linking maximum absorption to particle size

2.2.2 Physical QDs

QDs consist of a crystalline core, capped by a shell of larger bandgap material as shown in figure 2.4. This higher bandgap material shell is added to increase the depth of the potential well and to shield the core from environmental influences.

As a result, the also shell reduces the process called 'blinking'. While exciting quantum dots, an electron can 'jump' out of the quantum well. The QD will be charged positively. While the QD remains charged the energy configuration will not allow the the QD to be luminescent. As soon as another electron in captured in the well, the QD will start to luminesce again. The harder a QD is pumped, the more often this process will happen.

Also the QDs quality can decay in time. By oxidation of non-capped QD's the effective core size will decrease and the spectrum of the QD will shift towards the blue (blueing). Eventually the core can 'shrink' until a size that the particle is not luminescent any longer. This is called photobleaching.

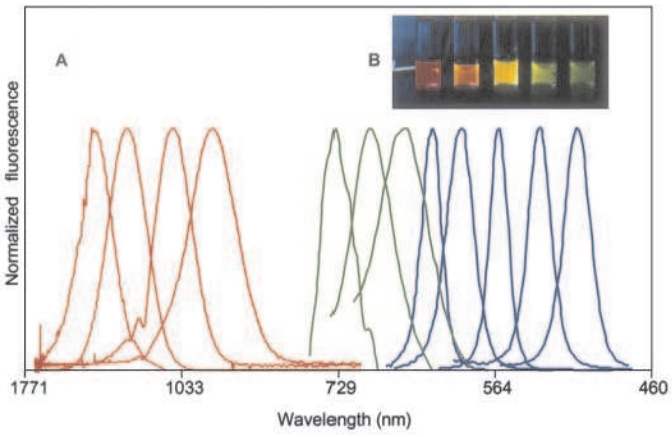

(A) Size- and material-dependent emission spectra of several surfactant-coated semiconductor nanocrystals in a variety of sizes. The blue series represents different sizes of CdSe nanocrystals with diameters of 2.1, 2.4, 3.1, 3.6, and 4.6 nm (from right to left). The green series is of In P nanocrystals with diameters of 3.0, 3.5, and 4.6 nm. The red series is of In As nanocrystals with diameters of 2.8, 3.6, 4.6, and 6.0 nm. (B) A true-color image of a series of silica-coated core (CdSe)-shell (Zn S or Cd S) nanocrystal probes in aqueous buffer, all illuminated simultaneously with a hand held ultraviolet lamp. [BMG+98]

Figure 2.10: Size- and material-dependent emission spectra of QDs

2.3 Radiative decay engineering

Radiative decay engineering is a term generally used when trying to modify the emission properties of luminescent systems, like quantum dots and atoms. Several mechanisms can modify the emission of a single emitter. First we will have a look at important parameteres of luminescence.

2.3.1 Important parameters

When comparing luminescent system there exist many parameters that give information on the most important fact for experimentalists: "how much light do I get out of my particle?".

Recalling figure 2.5 we see that there are two decay pathways: a radiative and a non-radiative. The natural radiative decay rate Γ is the rate at which photons would be emitted when no other decay rates would be present. It is the inverse of the natural lifetime τ_N of the excited state. However, there is also the non-radiative decay rate k_{nr}. Together they form the systems' lifetime τ_0 which gives an indication of the possible number of photocycles each second:

$$\tau_0 = \frac{1}{\Gamma + k_{nr}} \tag{2.4}$$

Another important parameter is the ratio between radiative and non-radiative de-

cays, called the quantum yield Q_0:

$$Q_0 = \frac{\Gamma}{\Gamma + k_{nr}} \tag{2.5}$$

The shorter τ_0 and the closer Q_0 is to 1, the more photons the system will give under the same excitation conditions.

Finally the apparent quantum yield Y tries to model the efficiency of emission from a particle. It refers to the intensity of a sample relative to a control sample. While keeping the illumination the same, one can either influence the local intensity L that excites the molecule, or the emission properties of the particle itself (Z):

$$Y = |L(\omega_{ex})|^2 \, Z(\omega_{em}) \tag{2.6}$$

2.3.2 Influencing luminescence

Several interactions between luminescent particles and metallic particles or surfaces exist. A metal can have effect on the excitation as well as the emission of a particle.

Local field enhancement

A small metal particle can locally enhance the electromagnetic field [NBX97]. It is greatly dependent on orientation of the electric field with respect to the particle, the particle size and the aspect ratio of the metal particle. The field can be enhanced by factors up to 3000. This effect can be explained by the incident light driving free electrons in the metal along the direction of polarisation. The alternating electron flow creates a oscillating charge density at the end of the particle, which on its turn creates an added local electric field.

Local field enhancement is just manipulating the emission intensity from a particle, since it only pumps the molecule harder. This will mean that neither Q_0 nor τ_0 are influenced, but only the number of photo cycles per second. The local field L is enhanced, so the apparent quantum yield Y will become larger.

Quenching

Quenching offers extra non-radiative decay channels. Quenching acts on very short (10nm) distances since it is associated with resonant energy transfer from the emitter to the metal. Therefore it is dependent on the cubed distance from the particle to the metal (d^3). The energy transferred to the metal is dissipated non-radiatively.

According to equations 2.4 and 2.5, both the lifetime and the quantum yield of the emitter will become lower. Also the apparent quantum yield will become lower.

Emission pattern

Also the detection efficiency of an experiment has to be considered. A nearby object can modify the emission field pattern as theoretically predicted by Novotny [Nov96] and experimentally confirmed by our group [GGPN$^+$00]. Figure 2.11 shows an emission pattern at an glass/air interface.

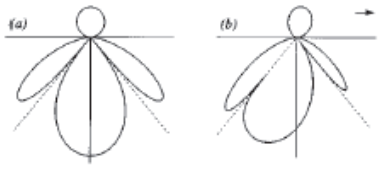

A molecule on a glass/air interface. a) No object present and b) The rim of a metal object is positioned just above the emitter.

Figure 2.11: Radiation patterns [Nov96]

As the object is positioned over an emitting molecule the radiation pattern will change. In case of an high ϵ-material the light emitted into the glass below will become less and the detection efficiency will decrease. This effect is not taken into account in the equation of apparent quantum yield.

Radiative decay enhancement

Lastly there is radiative decay enhancement. In this case the Jablonski diagram from fig. 2.5 is modified to the diagram in figure 2.12 by the presence of a metal colloid or surface.

An extra radiative decay Γ_m is added to the existing decay channels. Usually the non-radative decay added by the metal is taken by an increased $k_n r$. The parameters τ_0 and Q_0 will then become:

$$Q_m = \frac{\Gamma + \Gamma_m}{\Gamma + \Gamma_m + k_{nr}} \tag{2.7}$$

$$\tau_m = \frac{1}{\Gamma + \Gamma_m + k_{nr}} \tag{2.8}$$

This form of Q_m and τ_m influence the emission properties in a way that is very interesting if Γ_m is larger than the added k_{nr}. The quantum yield will increase, while the lifetime of the system will decrease!

The added radiative decay channel is a way to model a lower lifetime, using the equations defined before. The effect was predicted by the theory from Gersten en Nitzan [GN81]. Plasmons in a metal particle can be excited in resonance with the emission

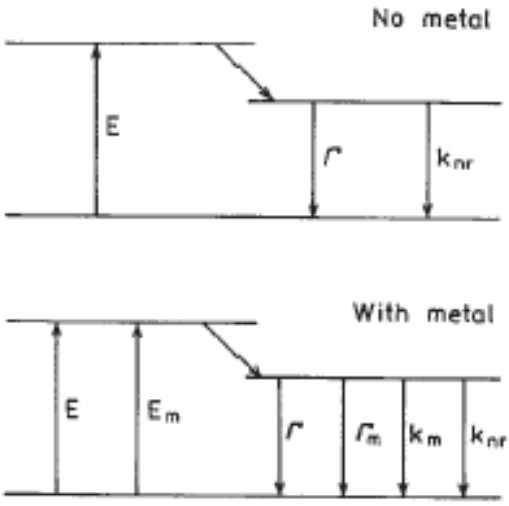

Figure 2.12: A metal in proximity to a luminescent system adds extra decay channels [Lak01]

dipole of the luminescent particle. These two dipoles have to be consider as one system with total dipole moment. From quantum mechanics we know that a larger dipole moment results in a shorter lifetime. Because the effect is dependent on plasmons, the enhancement factor largely depends on the particle size, shape and material.

Photonic mode density

On longer distances the radiative decay rate of an quantum emitter can also be influenced. This effect was first noted by Purcell [Pur46]. The emission of a photon by an quantum emitter requires the surrounding environment to support a photon mode. The strength of coupling depends on the density of these modes at the emission frequency. This concept is referred to as photonic mode density. Reflecting and absorbing surfaces may modify this density by imposing boundary conditions on the electromagnetic field. Oscillations of the lifetime with distance in front of an metal surface are the result of the phase of the reflected field at the emitter. If the reflected field is in phase with the source field emission is enhanced and lifetime is reduced; otherwise the emission is reduced.

2.3.3 Summary: studying radiative decay engineering effects with QDs

The (non-)radiative decay rate of quantum emitters is thus influenced by several processes that act at different distances. On the shortest distances, below 10nm, the metal is quenching the luminescence by dissipating the energy transferred from the emitter via

non-radiative decay pathways k_{nr}.

In the range of about 10nm to 50nm the enhanced excitation field E_m is pumping the system harder, by which only the apparent quantum yield will increase. This effect will not be observed in the experiment we perform since the excitation light has to polarised in such a way that the electrons in the metal are driven from and to the tip apex. In our case the polarisation of the excitation light is perpendicular to the tip, and no charge oscillations on the tip are to be expected.

In the same distance range, the coupling of the particle plasmon to the emitter will create a larger combined dipole moment, resulting in a shorter lifetime, which can be modelled by the added radiative decay channel Γ_m. This will increase the quantum yield, lower the lifetime of the system and increase the apparent quantum yield.

At distances in order of the emission wavelength the increase or decrease of photonic mode density through reflection of the emitted light by the metal. This will result in oscillations of the lifetime and quantum yield.

Quantum dots provide a powerful tool to study these effects. Since QD exciton decay has a longer lifetime than conventional luminescent dyes, effects on lifetime should be observed easily.

QDs do not have a fixed emission dipole, at least as long as the QD is spherical. Polarisation dependent effects which can be expected in radiative decay engineering could introduce polarised emission.

QDs show no or reduced bleaching, which enables time consuming scanning probe experiments.

Lastly, QDs show blinking behaviour. As shown in the article of Bawendi, this QD specific photophysical effect is influenced by changes in radiative lifetimes. The resulting competition between radiative and non-radiative decays of charged particles can effect into charged QD emission at slightly different wavelengths.

2.4 Single molecule luminescence microscopy

In general there are two ways to study luminescence of particles. In ensemble measurements large numbers of particles are studied, which leads to observation of average behaviour in an environment. This is the traditional method of luminescence microscopy. On the other hand there exist single molecule measurement techniques such as confocal microscopy and near-field scanning optical microscopy (NSOM). Single molecule experiments have become popular due to the advantages over traditional bulk experiments. Single molecule experiments reveal individual behaviour of molecules in an environment. This information may lead to a better understanding of a statistical average observed in bulk experiments. Secondly, it enables time resolved measurements on a single molecule, revealing intensity-, lifetime- and spectral fluctuations and among others.

To detect a single molecule one has to identify it between millions of other molecules. To be able to do so, one has to reduce background signal and optimise the detection efficiency of the set-up. Also, the concentration of molecules in the sample has to be small enough to avoid imaging of more than one particle at the same time.

The resolution of single molecule microscopy depends on the size of the focal spot. This size is limited by diffraction. When using a 1.4 NA oil immersion objective, measuring at a excitation wavelength of 568nm, the full width half maximum (FWHM) is $0.61\lambda/\text{NA} \approx 250\text{nm}$.

Using luminescence enhancement that is highly distance dependent one could improve on this resolution as shown in figure 1.3. The excitation focal spot would remain the same, but by modulating the emission properties in a distance dependent way one could introduce a substructure that results in a higher resolution.

Chapter 3

Experiment

In this chapter the experimental details of the measurement as mentioned in the introduction are described. First we cover the sample preparation, second the measurement apparatus, and finally the measurement procedure.

3.1 Sample preparation

A glass slide is cleaned by oxygen plasma etching to remove fluorescent material that is already present. QDs are then spin coated from solution onto the slide in different concentrations. We start with a concentration of 10^{-7}M of the stock solution. Each sample is diluted by a factor of ten. Samples with a concentration between 10^{-8} and 10^{-9} have a concentration that is suitable for single molecule experiments ($\approx$1 particle per μm^2).

The QDs used were made available through a collaboration with the group of Julius Vancso [Mat]. The QDs are made of a Cadmum-Selenide core and a Zinc-Sulfide shell. Their luminesence emission maximum is at 600nm and their size 6nm.

3.2 Measurement set-up

3.2.1 Confocal microscope

The measurements are performed using a inverted confocal microscope. The setup consists of four main parts: the excitation path, the objective with appropriate filter sets and the detection path.

Excitation path

The laser system used as a light source for the lifetime measurements consists of:
- A Spectra-Physics Millennia Xs laser;

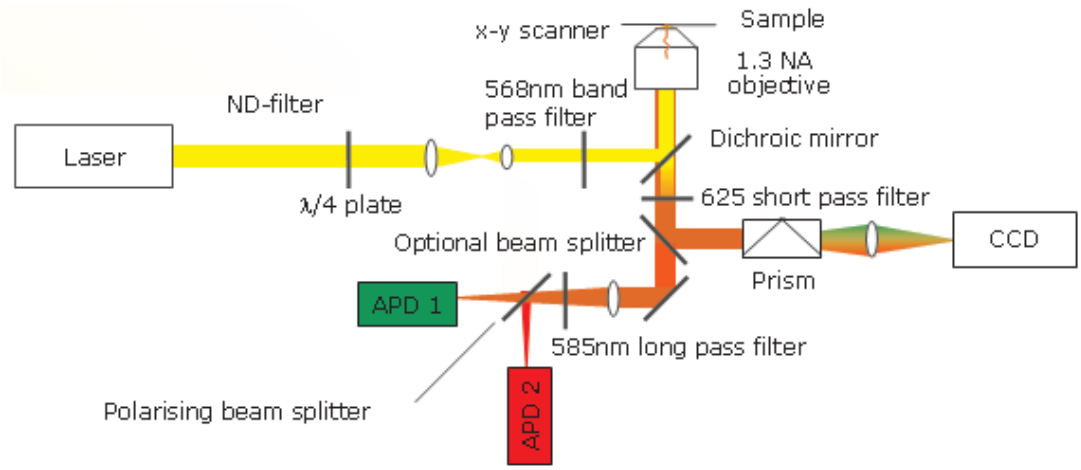

Figure 3.1: Confocal microscope setup

- a Spectra-Physics Tsunami Ti:Sapphire femtosecond pulsed laser;
- a Spectra-Physics Opal optical parametric oscillator (OPO);
- a LBO crystal;
- and an opto-acoustical modulator serving as a pulse selector.

The pump laser for the Ti:Sapphire laser is a Millenia Xs solid-state CW laser providing an input power of 9.5W at a wavelength of 532nm. The Ti:Sapphire laser generates pulses of about 100 fs at a repetition rate of 80MHz. It is operated at 750nm with an output power of about 1.6W. The OPO uses a temperature dependent non-linear LBO crystal as a gain medium. It's output wavelength is tuned at 1134nm with a power of about 90mW. These pulses are doubled to 568 nm by another LBO crystal. The pulse length increases significantly to about 300fs, however that is no problem for the experiment performed. As a final step the pulse selector brings down the repetition rate from 80MHz to 8MHz. The average power that is entering the confocal microscope has a maximum of about 5KW/cm^2. This is still more than enough for single molecule experiments.

Just before entering the set-up the beam is passing a beam expander which is used to block any higher order modes. The centre of the presumed Gaussian beam is selected to enter the microscope. Then the linearly polarised light is made circularly polarised using a $\lambda/4$-plate.

Filter set

The laserbeam is passing a 568nm bandpass filter and reflecting on a dichroic mirror that is reflecting light with a wavelength shorter than 580nm. The beam is focussed with a 1.4NA oil immersion objective onto the topside glass-air interface of the sample.

The fluorescence is collected using the same objective, now passing the dichroic mirror and a 625nm short pass filter, that filters out any light coming from the excitation laser or AFM laser on top.

Detection path

In the detection path the light is focussed by a lens and split by a polarising beam splitter. In this way both polarisations directions are directed to their own detector, which are avalanche photo detectors.

3.2.2 Atomic force microscope

The topographic information in the experiment is obtained by a atomic force microscope. An atomic force microscope (AFM) consists of a cantilever with a sharp tip at its end. A diode laser is reflecting on the tip and detected by a quadrant cell detector. In this way the angle of reflection can be determined. The tip is brought into close proximity of a sample surface. The force between the tip and the sample leads to a deflection of the cantilever. This deflection can be measured by changes in the angle of reflection of the diode laser.

The measurements are done in tapping mode. This means that the cantilever oscillates, vertically with respect to the sample surface, close to its resonance frequency. The tip of the cantilever will interact a short time with the surface during each oscillation period. From the amplitude of the oscillation the feedback adjusts the distance between the surface and the tip. The tip is scanned across the sample surface and the vertical displacement necessary to maintain a constant oscillation amplitude is recorded. The resulting map of this displacement represents the topography of the sample.

Using the AFM as interaction probe

In the AFM we use NSC15/Cr-Au cantilevers from Mikromasch [Mik]. These are silicon cantilevers which are gold coated, using an intermediate chromium layer to improve the gold adhesion. According to specifications, the tip radius of curvature is less than 50nm with a cone angle less than 30^o. The tips are coated at both sides to prevent strain problems.

The gold layer of the tip can be used as the nanometric metal object that influences the emission properties of the QDs. By scanning the surface, the tip-QD vector will change in length and orientation and therefore acts as a probe for the interaction between the tip and the QD.

3.2.3 Lifetime measurements

The lifetime measurements are done using a time correlated single photon counting (TCSPC) card. A molecule is excited periodically by a pulsed laser. Information of lifetime is collected over multiple excitation-emission cycles. The TCSPC card records the arrival time of every photon with respect to a synchronisation pulse of the pulsed laser. Because the probability of detecting one photon in one measuring period is less than one, every detected photon can be used to build the histogram of the arrival times as shown in figure 3.2.

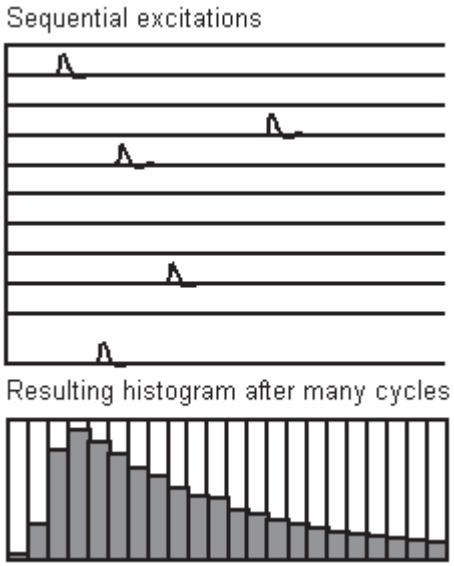

Figure 3.2: Time correlated single photon counting

The card measures the time of the photon with respect to a synchronisation pulse from the pulse selector. Usually the synchronisation pulse will arrive before the emitted photon. By adding wire between the pulse source and the TCPSC card we can delay the synchronisation pulse from the pulse selector. Now the synchronisation pulse will arrive *after* the photon. This is convenient since there will be many more synchronisation- than detection- pulses. For efficiency a time interval is started as a photon is detected and the interval is stopped as the synchronisation pulse is detected. In this way in time we will build a histogram that is reversed in time. This process is called time reversed TCSPC.

3.3 Measurement procedure

The measurement procedure consists of three parts. First the optics of the confocal microscope are aligned. Then the AFM tip has to be aligned with the optical paths and

finally the actual measurement is performed.

3.3.1 Alignment

To be able to perform the experiment, we have to put a QD and the AFM tip in the focus of the microscope. In this way we can detect the QD emission while influencing its properties with the AFM tip.

Aligning the optical part starts with optimising the excitation path. After this has been done, the detectors are aligned using a sample that is highly luminescent. This can either be a crowded QD sample or perylenes in a polymer matrix.

Once both the excitation and the detection paths have been optimised, the AFM is placed on top of the confocal microscope. The APD detection path is blocked and the filter set containing a short pass filter at 700nm is selected. In this way the AFM laser is blocked partially. Looking through the ocular (or observing the ocular camera) the AFM tip is positioned in the center of the field of view. Since the translation piezo's of the AFM have a working range of about 5μm most of the alignment has to be done manually. While the tip is scanning maximum range in tapping mode, the AFM head is slowly lowered and kept in the center of the field of view using the spindles. As the tip is in almost contact the spindles have to be handled very carefully. If the tip is drifting out of the center, one has to raise the head, move the tip in the opposite direction and approach again. Using the spindles while in contact can crash the tip very easily. As the distance between tip and sample becomes smaller, the tip will not only be seen because of the AFM laser, but also reflection patterns of the excitation throught the objective will appear. Finding the excact position of the tip with respect to the large cantilever is relatively easy. If the tip is in contact, and the focus is positioned just above the sample, a bright spot is observed at every pass of the tip. Also, the tip will have a moving Airy pattern that is interfering with the fixed Airy pattern of the sample slide. To put the tip within 10μm distance of the center of focus is not too hard to achieve. To prevent clipping of the AFM scanner during the measurements this distance has to be smaller than 5μm, which is a bit more problematic, but still feasible. Finishing the AFM alignment can be done by doing a reflection scan of the tip. The measurement filter set is selected, but this time without a long pass filter blocking the excitation light. As the AFM is scanned a ring-like pattern should appear. This ring pattern can be centered in the scan area, using the piezo offset in both x- and y-direction. After that the long pass filter has to be put back in the detection path.

3.3.2 Lifetime map

As the set-up has been aligned, the AFM tip is positioned as far as possible (5-7μm) from the focus, using the piezo offsets. The sample slide is scanned in one direction on

a line of about 10μm. Using the piezo offsets from the sample scanner a QD is selected and the signal is optimised. The sample scanner is stopped and the AFM tip is centred in the focus again.

Then the measurement is started. While the sample remains fixed (the selected QD remains in focus), the AFM tip is scanning the sample surface pixel by pixel. The scan usually consists of 128×128 pixels on a range of 1.5×1.5μm. The step size equals 11.7nm. The AFM tip stays on each pixel for 25 or 40ms to allow enough photons to arrive for the histogram. These values result in a total measurement time of about 22 minutes.

The QDs are illuminated using the pulsed laser at an power of about 300W/cm^2. Almost all measurement do not show bleaching of the QD, but off-times in the minute regime are frequently observed.

Chapter 4

Results and discussion

4.1 QD spectrum and size

Using a spectrometer we obtained the spectrum of the QDs in solution. Figure 4.1 shows an excitation spectrum (marked by dots) recorded at emission of 600nm while scanning the excitation wavelength. We observe three peaks. Starting from the right side there are two peaks at 585nm and 554nm, which are respectively associated with the heavy- and light- hole absorption on the lowest quantum ($n = 1$) level. The third peak at 492nm is associated with excitation to the second quantum level. This peak is marked as questionable since this part of the spectrum is largely corrected for the lines of the discharge lamp used for excitation.

The graph also shows an emission scan (marked by the squares) which records the emission spectrum while exciting the QDs at 488nm. The peak around a maximum of 601nm has a full width half maximum of 28nm. This width is twice as large compared to spectra obtained from single QDs, which have spectra that have a FWHM of about 15nm at room temperature. Since the emission spectra depend on size, this shows us that there exists a spread in sizes.

These spectra give information on the average size of the QDs, combining maximum of the spectrum at 585nm in the excitation scan. We can use this value in the theoretical and experimental curves relating QD size to the absorption maximum (shown in figure 2.9). These equations yield that the size of the core of the QDs is about 5.4nm.

This predicted size from the spectrum is confirmed by an AFM measurement on 134 QDs (figure 4.2). This measurement shows an average size between 6nm and 7nm. The difference from 5.4nm predicted from the spectral measurements can be explained by the ZnS shell that is around the CdSe core. This shell of several monolayers of ZnS, is not accounted for in the theory.

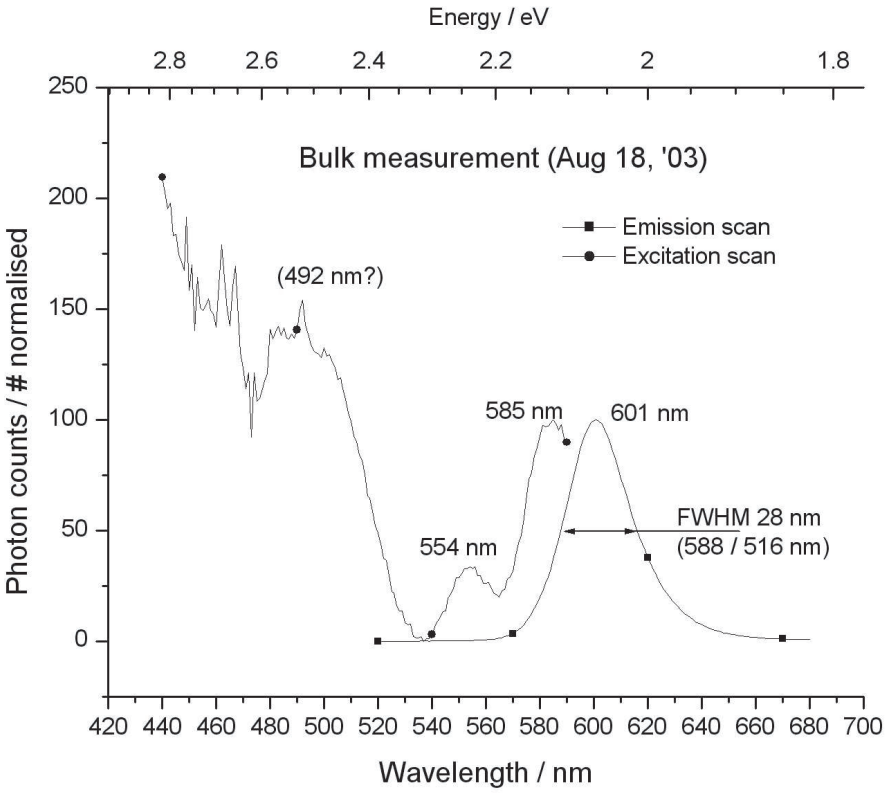

Figure 4.1: Dots: excitation scan recording emission at 600nm, squares: emission spectrum with excitation at 488nm

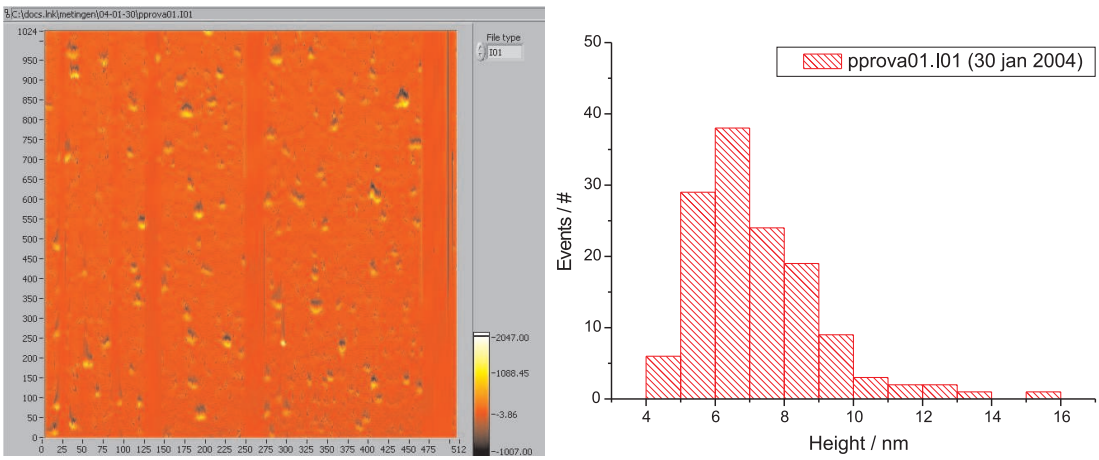

Figure 4.2: AFM image and statistics of the height of 134 QDs

4.2 Single QDs

All single QD measurements start with a sample scan of 10×10 or 5×5μm to locate individual dots. A typical image is shown in figure 4.3. The top left region contains almost no luminescent particles, while the rest of the scan is crowded, but contains single QDs. It has been very hard to prepare samples that have a continuous density of single QDs. As red and green in the image represent two orthogonal emission polarisation directions, this image shows that most, but not all, QDs do not show a polarised emission. One may think that no polarised emission is observed because of clustering of the QDs, but the discrete step blinking behaviour rules out this possibility. The blinking behaviour is very pronounced in these scans, since we use a high excitation power to be able to use a short integration time during these scan.

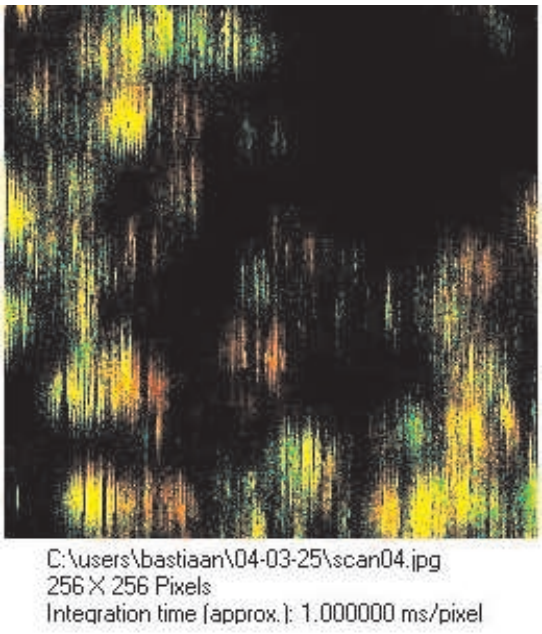

Figure 4.3: Sample surface scan of QDs. Excitation intensity approx. 5kW/cm^2, integration time 1ms.

After the scan has finished we select a single QD. The sample scanner then moves the selected point in the centre of the focus. The luminescence intensity of the QDs is followed in time. Single QD timetraces look very rough, as shown in figures 4.4 and 4.5. These two traces show the luminescence intensity of two different dots during a minute. The on-off behaviour is associated with blinking. All QDs show this behaviour, but all remain luminescent for over a minute, even at powers in the kW/cm^2 regime. If the excitation power is large the blinking behaviour becomes more pronounced (figure 4.4), consistent with reports of others [SNL$^+$01]. At lower excitation powers (figure 4.5) the effect is seen as well. In this case most of the off-times can be shorter than the

binning time, and no discrete behaviour is seen, but rather a continuous fluctuation in luminescence intensity.

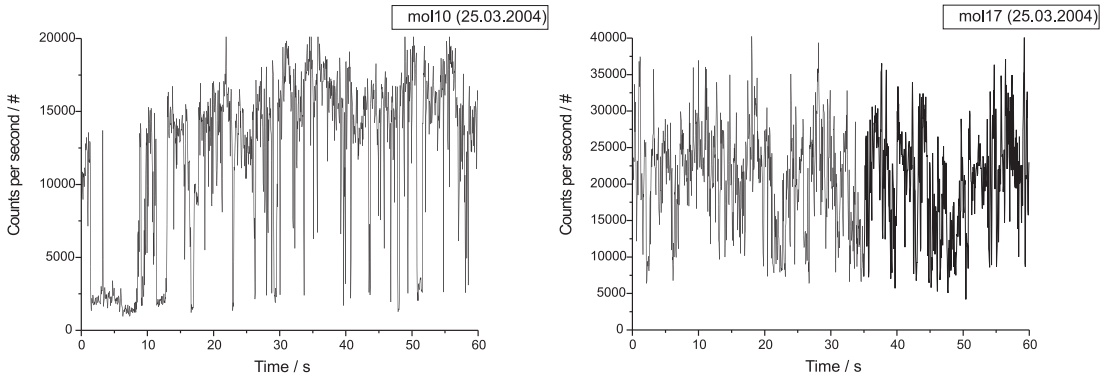

Figure 4.4: QD timetraces (60 seconds, excitation power 4kW/cm^2, 568nm)

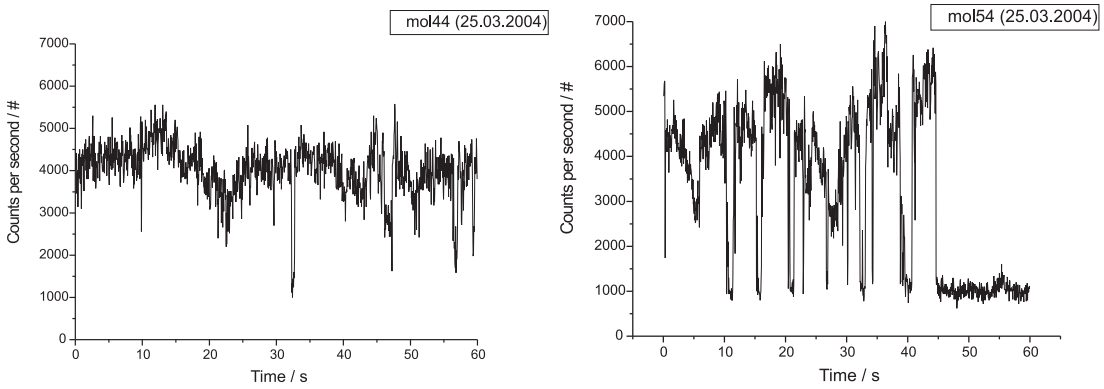

Figure 4.5: QD timetraces (60 seconds, excitation power 300W/cm^2, 568nm)

During the timetraces also the arrival times of the photons have been recorded. The histograms created from the arrival times of the QDs in the right half of the previous figures are shown in figure 4.6. They have been fitted with a bi-exponential decay curve. The relative strength of either of the two exponential decays can vary from almost only one fast decay component (from 2ns to 4ns), to almost only one slow decay component (from 20ns to 25ns). This can be explained by a distribution in the quality of the QD. Fast decay is associated with emission from surface defects, competing with the electron-hole recombination emission from the QD core as reported in [WZKM00] and [SBPM02]. In figure 4.7 we observe the statistics of 105 QD lifetimes.

The long lifetimes, blinking behaviour but no photobleaching, non-polarised emission and the recorded spectra (not shown) confirm that we are indeed studying single quantum dots.

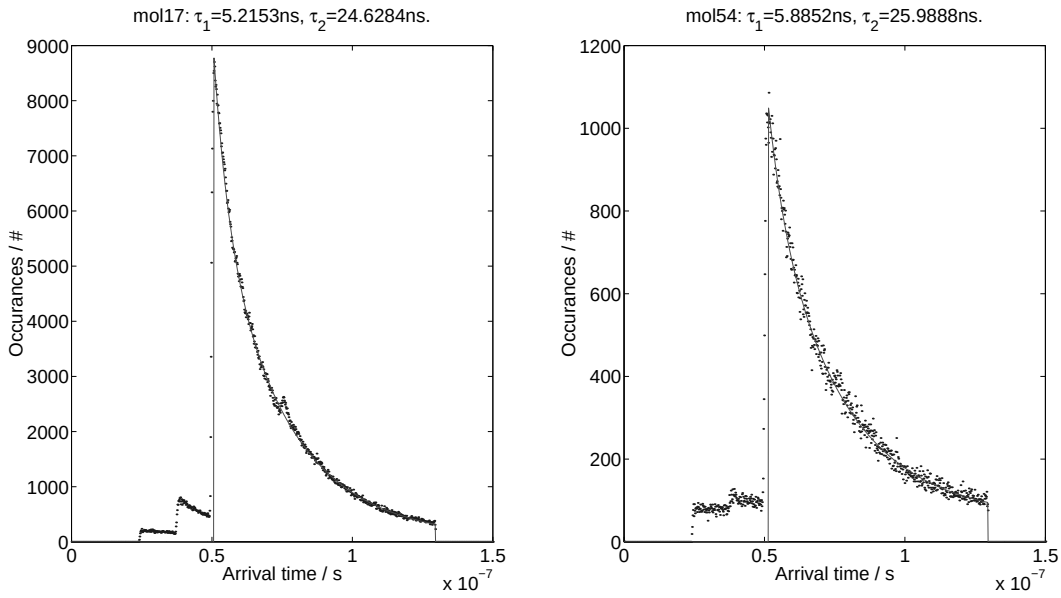

Figure 4.6: Histogram of photon arrival time for two different dots at high (left) and low (right) excitation power.

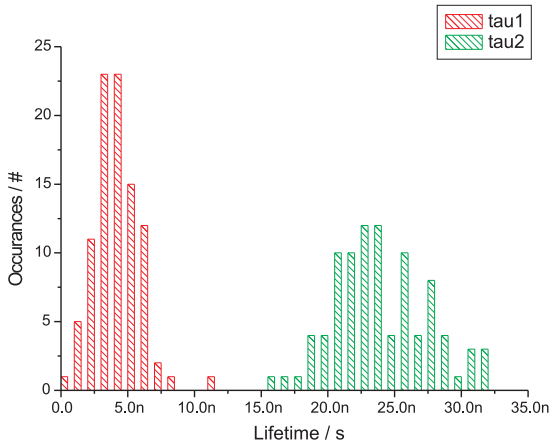

Figure 4.7: Lifetime of 105 QDs recorded for 1 minute

4.3 Combined confocal and AFM

After the initial measurements on single QDs using either AFM or confocal microscope, we continued to the next step: combining the two measurement methods. First we did measurements using a Silicon-Nitride tip, although we knew from other experiments in our group that these tips are luminescent. Unfortunately, as expected, this luminescence was completely dominant over the luminescence of the QDs. Another issue was that these tips are not suited for tapping mode AFM because of their low spring constant. Tapping mode AFM is needed for the measurements since the QD on the sample surface are not well fixed and contact mode AFM could drag them around during the measurements. The results of these measurements have not been included in this report.

4.3.1 Uncoated Si tip

Combined AFM and confocal measurements on single QDs using a Si tip were first performed to master the set-up and alignment procedure, but gave already interesting results. Figure 4.8 shows an image of the most promising experiment. On the left side we see the luminescence intensity of one single QD followed in time, recording line by line from left to right. Also this image is representing the luminescence intensity as a function of position of the AFM tip. The stripy pattern result from the blinking behaviour of the QD. On the right side the intensity is decreasing most probably because the focus of the confocal is drifting away from the QD. Besides that we observe in the intensity image a dark triangular pattern that is reproducing over several lines. Since the only parameter changing in this image is the position of the AFM tip with respect to the QD in the focus of the confocal microscope. Therefore we conclude that the QD is positioned in the centre of this pattern. As the AFM tip is positioned on top of, or close to the QD, the luminescence intensity clearly decreases. The triangular pattern can be explained by the tip shape. This three sided pyramidal tip has been scratched on the surface, and therefore has a triangular tip edge, which is confirmed by the AFM height image that is shown on the right side of figure 4.8. The image also suggests that more than one QD is observed since the structure is higher than the surrounding structures.

The local decrease of intensity can be explained by the a modified emission pattern combined with quenching. Since silicon is a high index material, the emission pattern will partially be drawn into the tip and therefore the detection efficiency goes down as the tip is over the QD. At the edges of the tip the intensity seems to increase, which can also be explained by modification of the emission pattern. However, this effect also could be the result of reflection of excitation light towards the QD and increased QD excitation.

Local field enhancement effects will not be in effect, since a blunt tip is used and the polarisation direction of the excitation light is perpendicular to the tip apex.

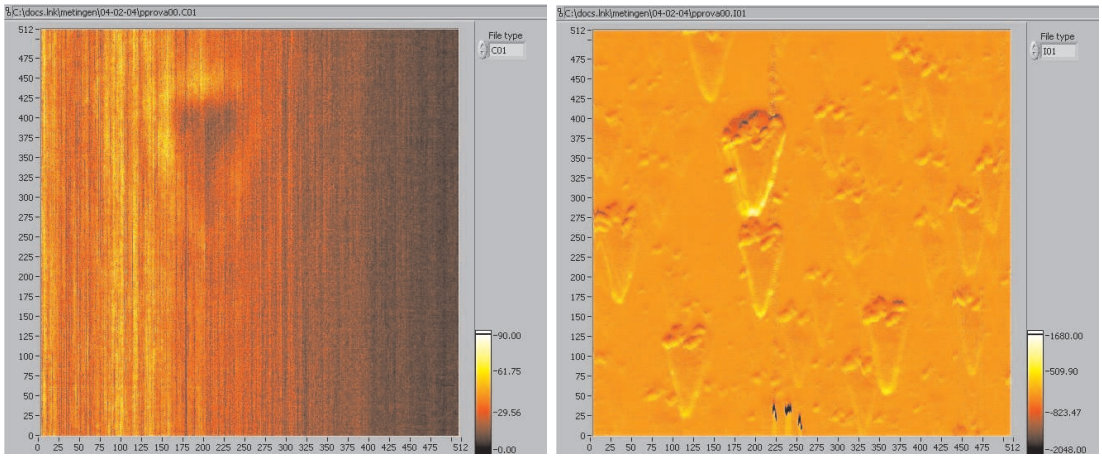

Area 3.5×3.5μm

Figure 4.8: Influence on luminescence (left) correlated with topography (right)

Effects on lifetime have not been recorded, since the data acquisition program was not optimised yet and could not handle the count rate in the brighter areas.

4.3.2 Gold coated tip

After the measurements with an uncoated tip, we proceeded to work with the gold-coated Si tips. The first measurements were performed on a small scan area of 500×500nm, to obtain a high spatial resolution. These measurements did not show patterns of local decrease of intensity. The reason of this absence is not clear. Although the alignment procedure was the same as the successful measurements later, it could be that the alignment on such a small scale have not been accurate enough. After increasing the scanning area to 2×2 or 1.5×1.5μm intensity patterns were visible.

In figure 4.9 we see an intensity plot of a measurement that does show a concentric ring-like intensity pattern on distances comparable to the wavelength of light. The area in this scan is 2×2μm. Left side of the figure shows the raw data obtained, while the image on the right has been smoothed with a Gaussian filter to ease the recognition of the pattern.

The right side of the scan is completely dark since the emitter has photobleached. It is unlikely that this emitter is a QD, since the histogram of arrival times obtained could be fitted by a single exponential decay with a lifetime of 2ns. Besides that no noticeable blinking is observed, in contrast to all other measurements. This measurement is included since it is the nicest image illustrating the influence of the tip. The centre of the pattern, just below the centre of the image marks the position of the emitter with respect to the AFM scanner.

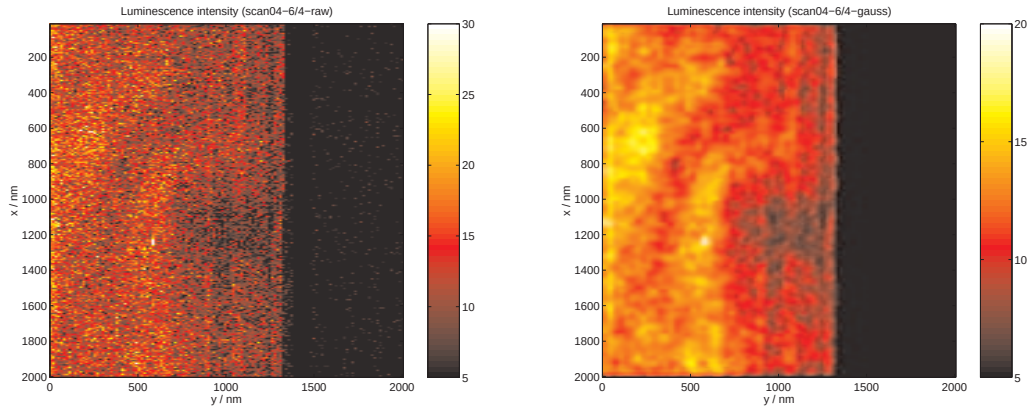

Left: Raw intensity data, right: Smoothed by a gaussian filter

Figure 4.9: Oscillating luminescence intensity

In the next figure 4.10 we see a measurement on a QD. The blinking behaviour of the QDs is easily seen. This image is again acquired scanning the AFM tip line by line from top to bottom and reverse. This explains the stripy patterns from the blinking behaviour. In spite of these lines we observe a pattern in the lower right part of the scan. There is a light ring, surrounding a dark ring with a bright spot in the centre,

reproducing over several lines. Since the AFM tip position is the only parameter varying, we can ascribe this pattern to AFM tip position. The left image is showing raw data, while the right image is smoothed by a Gaussian filter to ease the recognition of the pattern.

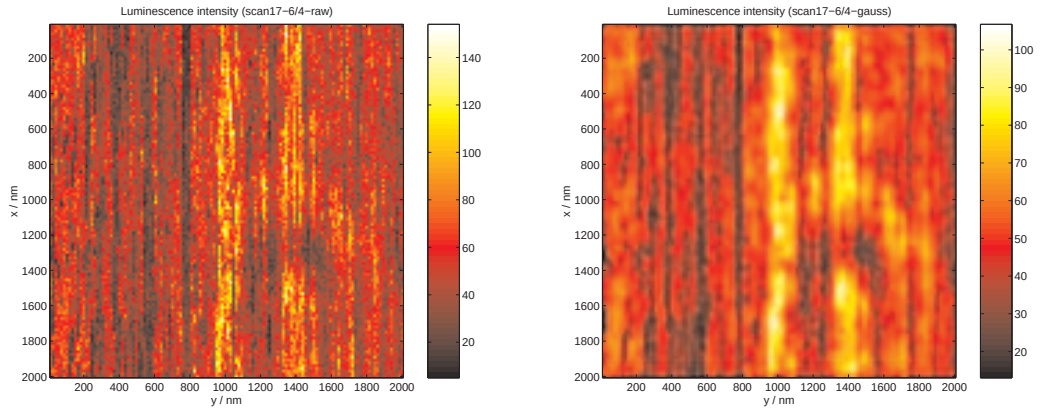

Left: Raw intensity data, right: Smoothed by a gaussian filter. Scan size $2\times2\mu$m, excitation power 300W/cm^2 at 568 nm, emission recorded between 585nm and 625nm, integration time 40ms per pixel

Figure 4.10: Concentric ring pattern in luminescence intensity of a QD

Figure 4.11 shows a zoom of the interesting area in this measurement. It has been smoothed by a Gaussian filter of 5x5 pixels, and the histograms have been combined likewise to create histograms that have enough structure to fit a single exponential function. The histograms themselves do not contain enough counts although the integration time in these experiments has been 40ms. The count rate of a single QD is not high enough to build a reliable histogram in this integration time, but there has to be a trade off between the total measurement time, the number of pixels, and the integration time.

The single exponential fits means that the numeric value of associated lifetime is not meaningful, since a double exponential decay should have been fitted. The relative value however can tell about the qualitative lengthening or shortening of the decay lifetime.

The image on the right is the lifetime of the exponential decay curve fitted to each pixel histogram. Although the image is very rough, a correlation between luminescence intensity and lifetime can be observed. A radial integral in this image as shown in 4.12, shows a clear correlation between count rate and lifetime. This suggest that interference of the excitation light is not the sole origin of the intensity modulation.

The blinking behaviour also shows influence on the lifetimes that are associated with the histograms. If the QD is in a 'bright' period, the lifetime raises. This increase of emission rate combined with a long lifetime has been also reported in literature [SBPM02].

An even closer look at the bright spot as shown in figure 4.13 suggests a higher intensity at the edges of the bright spot. This would be on a distance of about 50nm

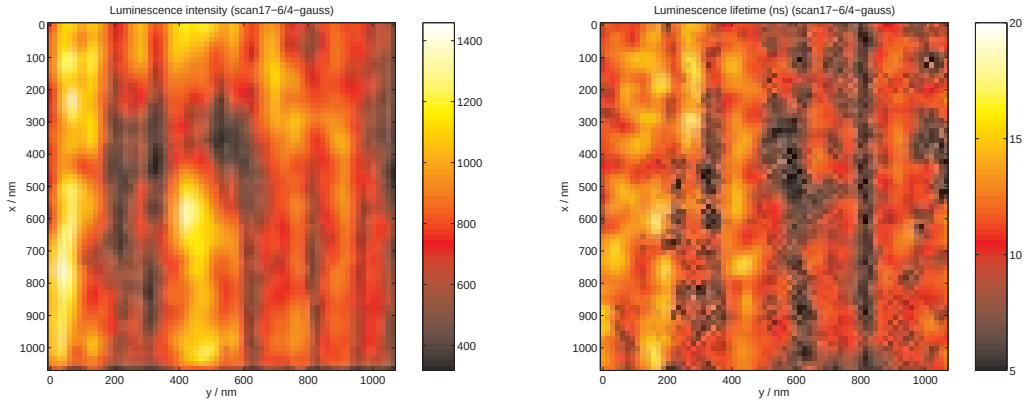

Zoom of scan in figure 4.10. Left: intensity, right: lifetime.

Figure 4.11: Zoom of concentric ring pattern in luminescence intensity

from the centre of the pattern. Also the centre of the bright spot seems to be a bit less intense.

Summarising; the images shown in figures 4.10, 4.11 and 4.13 clearly show a intensity pattern that is dependent on the QD-tip distance. Unfortunately the fitted lifetimes are not numerically significant, but they do show a trend. From the intensity pictures we can conclude that at distances comparable to the wavelength of the light we see an effect that has a period of the wavelength of the excitation or emission light. The data is not clear enough to discriminate which of the two. Therefore this modulation could be due to either an interference which leads to an oscillating pumping rate, or a oscillating photonic mode density. From the lifetime it is hard to pinpoint the main process, since the effects in lifetime are also influenced by the QD and it near environment itself. The 1st quadrant of the dark ring and the oscillating lifetime on the vertical line at 600nm suggest that there is at least some influence on the photonic mode density.

The pattern will not be significantly influenced by a change in detection efficiency because of a modified emission pattern since the tip in all cases is far away from the QD.

The bright spot in the centre suggests enhanced (non reduced) emission from the quantum dot. Just as the larger rings, both an increase in excitation rate and photonic mode density can play a role.

The bright ring at the edge and the darker central part of the spot suggest that in the centre of the spot the AFM tip enters the quenching range. Unfortunately the lifetime image does not give additional information in this area.

Regarding these conclusions we have to consider our tapping mode experiment. On each pixel the lateral position of the tip with respect to the QD is fixed. However, the vertical QD-tip distance is oscillating at a frequency of 260kHz. The tapping amplitude

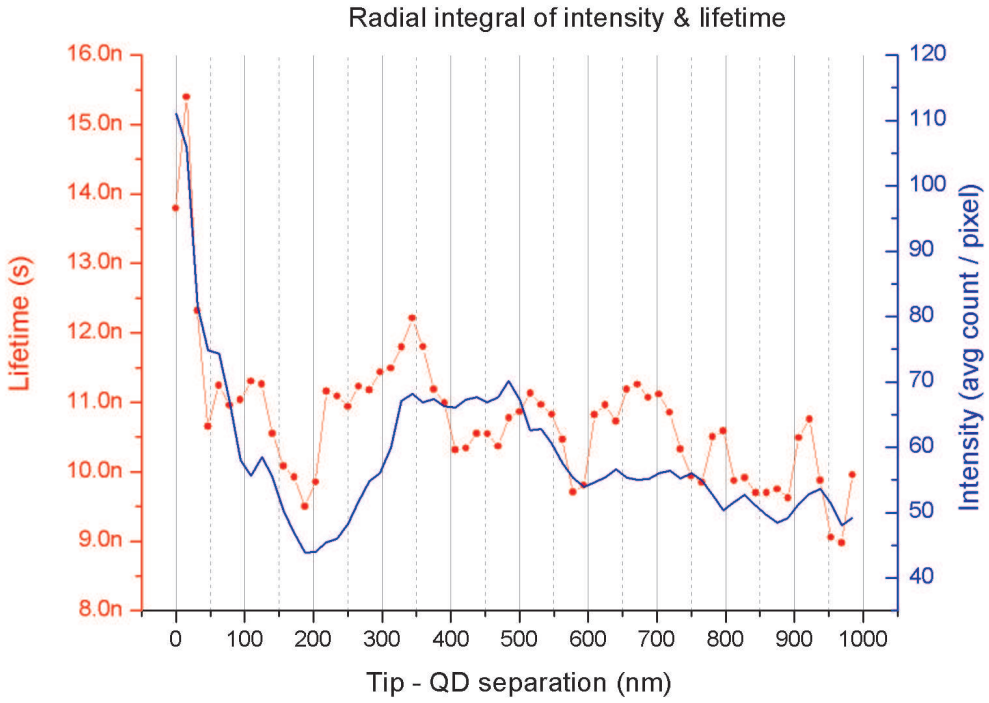

Figure 4.12: Linetrace through radial integral in the image of figure 4.11

is unknown, but supposed to be in the range of 20-200nm. This means that if the tip is positioned on top of the QD the time spent in the quenching regime is only short. This could explain that no significant quenching is observed in the central bright spot. The time in the enhancement regime and the time of no or just slight influence are longer and result in an enhanced emission. This assumption could be proven by performing experiments with time gating for the lower and upper half of the AFM tip oscillation while detecting the emission. Such experiments has been performed, with results that confirm this assumption.

The dark and bright rings will be less influenced by the oscillating AFM tip, since the photonic mode density and excitation rate do not depend on the exact tip-QD distance. This is confirmed by another measurement. In this measurement the tapping amplitude of the AFM tip was higher by a factor of 2. The image in figure 4.14 also shows a ring like pattern. This pattern is much harder to detect, since the tapping amplitude is larger. Now the tip is presumably oscillating through both enhancement as reduction regime.

Furthermore, the centre of this pattern does not show a bright spot. This can be explained by the tip tapping mostly in the region of decreased photonic mode density / excitation rate.

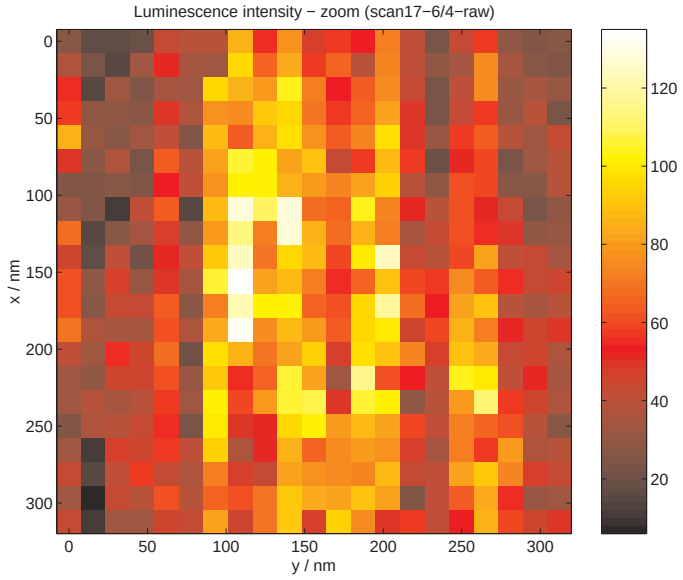

Zoom of scan in figure 4.11

Figure 4.13: Zoom of bright spot in luminescence intensity

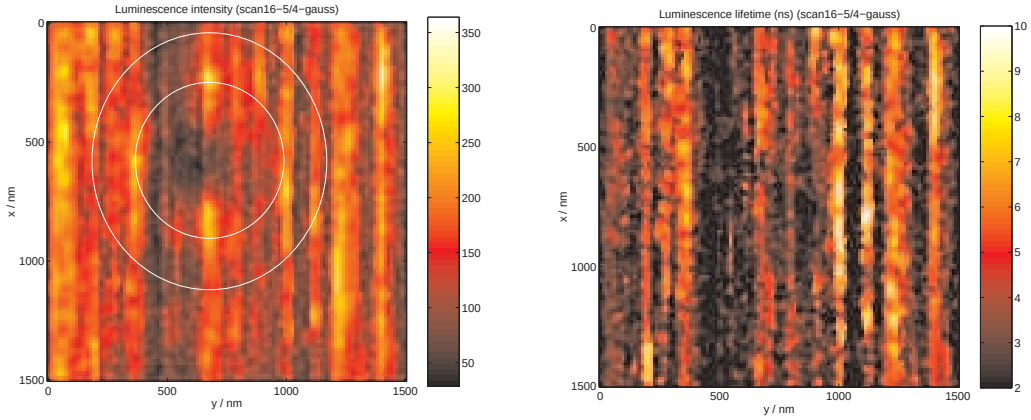

Left: intensity, right: lifetime

Figure 4.14: Luminescence intensity and lifetime modulation with higher tapping amplitude

4.4 Conclusion

From the measurements performed we can conclude that we can observe luminescence intensity modulation by an AFM tip. Using a dielectric tip we observe a decreased luminescence intensity as the tip is positioned on top of the QD. This effect is mainly associated with a lower detection efficiency because of a modified emission pattern. Since lifetime has not been recorded, we cannot draw final conclusions from this measurement in terms of a quenching contribution.

In the measurements with a gold-coated tip, the most pronounced effect is seen on distances comparable to the wavelength of the light. This modulation is associated with a modification in photonic mode density which increases (decreases) the emission intensity by stronger (less strong) coupling of the emission dipole to the radiation field or interference of the excitation field, which influences the pumping rate of the QD. The latter cannot be solely responsible for the effect, since also the lifetime is clearly modulated. This lifetime is also changing because of competition of radiative and non-radiative processes of the QD.

In the measurement with the uncoated tip, the oscillating luminescence intensity was not observed. This is expected from theory on photonic mode density, which predicts the oscillating character just for reflecting surfaces. Interference effects will also be different for both tips, so we cannot pinpoint the main effect.

On distances shorter than 100nm, we see an effect that is dependent on tapping amplitude of the AFM tip. If this amplitude is high, the emission remains reduced in this area. This can be explained by a tip that is oscillating most of the time in the regime of a decreased photonic mode density or excitation rate. A modified emission pattern may also play a role. Since the first measurements on an area of 500×500nm were performed using a large tapping amplitude, it is understood why no effects were observed.

Using a smaller tapping amplitude on these distances results in a bright spot in the centre of the pattern. This spot can be explained by an enhanced emission from the quantum dot because the tip spends enough time in the enhancement regime. An optimistic view shows a bright ring on the edge, and a darker area in the centre of the bright spot, which can be explained by respectively remaining outside or entering the quenching regime. Again we cannot draw conclusion on the origin of this enhancement, since the lifetime data is not accurate enough.

Altogether, these experiments show that we can influence the luminescence of a QD using a AFM tip. A dielectric tip results in a locally decreased emission intensity, while a gold-coated tip shows an periodic enhancement or reduction of emission intensity on the length scale of the wavelength. More accurately obtained lifetime data could indicate the main process.

On the shortest distances, we can conclude that it is important to do time-gated experiments and use the smallest tapping amplitude feasible, to reduce the influence of the oscillating distance between QD and tip.

Besides that, another trade off should be made between integration time, scan size and number of pixels. Future experiments could consist of a introductory measurement to obtain rough intensity information, set to cover $1.5\times1.5\mu$m using 128x128pixels and an integration time of 10ms. Then the central area should be studied more extensively, using a smaller scan size (like 100×100nm or a rectangular area of 200×50nm), a smaller number of pixels and longer integration time to obtain enough counts for the time histograms. If the alignment is stable and accurate, also measuring on just a single central line, and thus reducing the number of pixel greatly, would be an excellent method.

Bibliography

[AB99] R.M. Amos and W.L Barnes. Modification of spontaneous emission lifetimes in the presence of corrugated metallic surfaces. *Physical Review B*, 59(11):7708–14, 1999.

[AM76] N.W. Ashcroft and N.D. Mermin. *Solid State Physics*. Thomson Learning, 1976.

[BMG+98] M. Bruchez Jr, M. Moronne, P. Gin, S. S. Weiss, and A.P. Alivisatos. Semiconductor nanocrystals as fluorescent biological labels. *Science*, 281:2013–2016, 1998.

[Bos] Boston electronics. Website. http://www.boselec.com/.

[Bru84] L.E. Brus. Electron-electron and electron-hole interactions in small semiconductor crystallites: The size dependence of the lowest excited electronic state. *Journal of Chemical Physics*, 80(9):4403–09, 1984.

[Ene] Energy and semiconductor research (ehf) laboratory, university of oldenburg. Website. http://ehf.uni-oldenburg.de/pv/nano/.

[ENSB99] S.A. Empedocles, R. Neuhauser, K. Shimizu, and M.G. Bawendi. Photoluminescence from single semiconductor nanostructures. *Advanced Materials*, 11(15):1243–56, 1999.

[Gam65] George Gamow. *Mr. Tompkins in Paperback*. Cambridge University Press, 1993 edition, 1965.

[Ger99] Henkjan Gersen. A dipolar light source in nsom. Master's thesis, Optical Techniques, University of Twente, April 1999.

[GGPN+00] H. Gersen, M.F. Garcia-Parajo, L. Novotny, J.A. Veerman, L. Kuipers, and N.F. van Hulst. Influencing the angular emission of a single molecule. *Physical Review Letters*, 85(25):5312–15, 2000.

[GMS94] Michel Goossens, Frank Mittelbach, and Alexander Samarin. *The LaTeXCompanion*. Addison-Wesley, 1994.

[GN81] J. Gersten and A. Nitzan. Spectroscopic properties of molecules interacting with small dielectric particles. *Journal of Chemical Physics*, 75(3):1139–52, 1981.

[GP] M. García-Parajó. Semiconductor quantum dots. Lecture notes.

[Hep] Carl Hepburn. Britney's guide to semiconductor physics. Website. http://britneyspears.ac/.

[Koo01] Marjolein Koopman. Single molecular fingerprints of the red autofluorescent protein dsred. Master's thesis, Optical Techniques, University of Twente, June 2001.

[Kri01] Arco Krijgsman. Single molecular needlework. Master's thesis, Optical Techniques, University of Twente, September 2001.

[KSY+02] O. Kulakovich, N. Strekal, A. Yaroshevich, S. Maskevich, S. Gaponenko, I. Nabiev, U. Woggon, and M. Artemyev. Enhanced luminescence of cdse quantum dots on gold colloids. *Nano Letters*, 2(12):1449–52, 2002.

[Lak01] J.R. Lakowicz. Radiative decay engineering: Biophysical and biomedical applications. *Analytical Biochemistry*, 298:1–24, 2001.

[Mat] Materials science and techology of polymers, university of twente. Website. http://mtp.ct.utwente.nl/.

[Mik] Mikromasch. Website. http://www.spmtips.com/.

[NBX97] L. Novotny, R.X. Bian, and X.S. Xie. Theory of nanometric optical tweezers. *Physical Review Letters*, 79(4):645–48, 1997.

[Nov96] L. Novotny. Single molecule fluorescence in inhomogeneous environments. *Applied Physics Letters*, 69(25):3806–8, 1996.

[Pee99] C. Peeters. Quantum dots, optical properties of semiconductor nanocrystals. Report, October 1999.

[Pur46] E.M. Purcell. Spontaneous emission probabilities at radio frequencies. *Physical Review*, 69(11-12):681, 1946.

[Qua] Quantumdot company. Website. http://www.qdots.com/.

[SBPM02] G. Schlegel, J. Bohnenberger, I. Potapova, and A. Mews. Fluorescence decay time of single semiconductor nanocrystals. *Physical Review Letters*, 88(13):137401, 2002.

[SNL+01] K.T. Shimizu, R.G. Neuhauser, C.A. Leatherdale, S.A. Empedocles, W.K. Woo, and M.G. Bawendi. Blinking statistics in single semiconductor nanocrystal quantum dots. *Physical Review B*, 63(20):205316, 2001.

[SWF+02] K.T. Shimizu, W.K. Woo, B.R. Fisher, H.J. Eisler, and M.G. Bawendi. Surface-enhanced emission from single semiconductor nanocrystals. *Physical Review Letters*, 89(11):117401–1, 2002.

[Wik] Wikipedia, the free encyclopedia. Website. http://wikipedia.org/.

[WZKM00] F. Wu, J.Z. Zhang, R. Kho, and R.K. Mehra. Radiative and nonradiative lifetimes of band edge states and deep trap states of cds nanoparticles determined by time-correlated single photon counting. *Chemical Physics Letters*, 330:237–42, 2000.